Myosin phosphatase is inactivated by caspase-3 cleavage and phosphorylation of myosin phosphatase targeting subunit 1 during apoptosis

Takahiro Iwasaki[a], Takeshi Katayama[b], Kazuhiro Kohama[b], Yaeta Endo[a,c,d], and Tatsuya Sawasaki[a,c,d]
[a]Cell-Free Science and Technology Research Center and Venture Business Laboratory, Ehime University, Matsuyama, Ehime 790-8577, Japan; [b]Department of Molecular and Cellular Pharmacology, Gunma University Graduate School of Medicine, Maebashi, Gunma 371-8511, Japan; [c]Proteo-Medicine Research Center, Ehime University, Toon, Ehime 791-0295, Japan; [d]RIKEN Systems and Structural Biology Center, Yokohama, Kanagawa 230-0045, Japan

ABSTRACT **In nonapoptotic cells, the phosphorylation level of myosin II is constantly maintained by myosin kinases and myosin phosphatase. During apoptosis, caspase-3–activated Rho-associated protein kinase I triggers hyperphosphorylation of myosin II, leading to membrane blebbing. Although inhibition of myosin phosphatase could also contribute to myosin II phosphorylation, little is known about the regulation of myosin phosphatase in apoptosis. In this study, we have demonstrated that, in apoptotic cells, the myosin-binding domain of myosin phosphatase targeting subunit 1 (MYPT1) is cleaved by caspase-3 at Asp-884, and the cleaved MYPT1 is strongly phosphorylated at Thr-696 and Thr-853, phosphorylation of which is known to inhibit myosin II binding. Expression of the caspase-3 cleaved form of MYPT1 that lacked the C-terminal end in HeLa cells caused the dissociation of MYPT1 from actin stress fibers. The dephosphorylation activity of myosin phosphatase immunoprecipitated from the apoptotic cells was lower than that from the nonapoptotic control cells. These results suggest that down-regulation of MYPT1 may play a role in promoting hyperphosphorylation of myosin II by inhibiting the dephosphorylation of myosin II during apoptosis.**

Monitoring Editor
J. Silvio Gutkind
National Institutes of Health

Received: Sep 1, 2011
Revised: Dec 3, 2012
Accepted: Jan 15, 2013

INTRODUCTION

Apoptotic cell death is an indispensable process for embryonic development and maintenance of tissue homeostasis in multicellular organisms (Jacobson *et al.*, 1997). Abnormal cell proliferation caused by the loss of apoptosis leads to tumor development, autoimmune diseases, and viral infections, whereas excessive apoptosis results in inadequate cell loss disorders, such as neurodegenerative diseases, and cardiovascular diseases (Wolf *et al.*, 2001; Karin and Lin, 2002; Savill *et al.*, 2002; Friedlander, 2003; Mercer and Helenius, 2008). To protect against these severe apoptotic defects, apoptosis is strictly regulated by caspase-mediated signaling cascades. Caspase is a member of the cysteine-specific aspartate protease family, which is responsible for producing various apoptotic events by cleaving apoptosis-specific substrates. Among 12 identified mammalian caspases (Ghavami *et al.*, 2009), caspase-3 is referred to as the executioner caspase that triggers the lethal processes associated with apoptosis, including cell shrinkage, nuclear degradation, membrane blebbing, and apoptotic body formation, by cleaving focal adhesion kinase, lamin B, and Rho-associated protein kinase I (ROCK-I), respectively (Levkau *et al.*, 1998; Coleman *et al.*, 2001; Slee *et al.*, 2001). ROCK-I and its substrate, myosin II, play particularly critical roles in producing the morphological changes in

This article was published online ahead of print in MBoC in Press (http://www.molbiolcell.org/cgi/doi/10.1091/mbc.E11-08-0740) on January 23, 2013.

Address correspondence to: Tatsuya Sawasaki (sawasaki@ehime-u.ac.jp).

Abbreviations used: CHX, cycloheximide; DMSO, dimethyl sulfoxide; FITC, fluorescein isothiocyanate; GST, glutathione *S*-transferase; HRP, horseradish peroxidase; IgG, immunoglobulin G; MP, myosin phosphatase; MRLC, myosin regulatory light chain; MYPT1, myosin phosphatase targeting subunit 1; PBS, phosphate-buffered saline; PP1, protein phosphatase 1; ROCK-I, Rho-associated protein kinase I; siRNA, small interfering RNA; TNF, tumor necrosis factor-α; ZIPK, zipper-interacting protein kinase

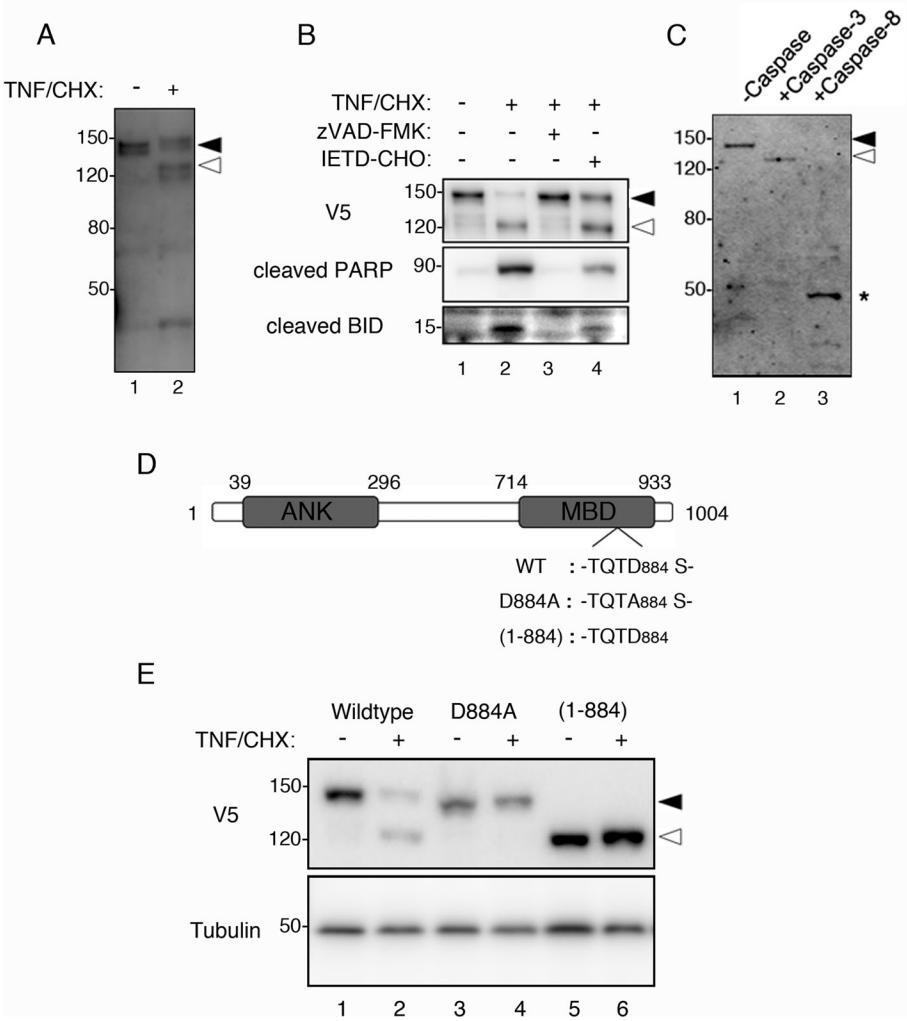

FIGURE 1: Caspase-3–mediated cleavage of MYPT1 during apoptosis. (A) Cleavage of endogenous MYPT1 in apoptotic cells. HeLa cells were treated with dimethyl sulfoxide (DMSO) or TNF/CHX for 3 h. Total cell lysates were immunoblotted with anti-MYPT1 antibody. (B) Inhibition of MYPT1 cleavage. HeLa cells were transiently transfected with V5-MYPT1-WT. At 24 h after transfection, the cells were treated with DMSO, TNF/CHX, TNF/CHX zVAD-FMK, or TNF/CHX/IETD-CHO for 3 h. Total cell lysates were immunoblotted using anti-V5 antibody (top panel), cleaved PARP antibody (middle panel), or BID antibody (bottom panel). (C) Identification of MYPT1-cleaving caspase. FLAG-MYPT1 was treated with caspase-3 or caspase-8 at 30°C for 1 h in vitro. Cleavage of MYPT1 was analyzed by immunoblot assay using the anti-FLAG antibody. Asterisk indicates the caspase-8–cleaved form of MYPT1. (D) Schematic representation of MYPT1. ANK, ankyrin repeat; MBD, myosin-binding domain. The caspase-3 cleavage site TQTD884 was identified by amino acid sequencing. D884A and (1-884) indicate the caspase-3 cleavage site mutant and the caspase-3–cleaved form of MYPT1 (lacking the C-terminal end), respectively. (E) In vivo cleavage of MYPT1 at Asp-884. HeLa cells transfected with V5-MYPT1-WT, V5-MYPT1-D884A, or V5-MYPT1-(1-884) were treated with DMSO or TNF/CHX for 3 h. Total cell lysates were immunoblotted using anti-V5 antibody (top panel) or anti–α-tubulin antibody (bottom panel). Positions of the full-length and caspase-3–cleaved MYPT1 are indicated using filled and open arrowheads, respectively. Positions of molecular weight standards are indicated in kilodaltons on the left.

apoptotic cells. The activity and localization of myosin II in vivo is regulated by phosphorylation of the myosin regulatory light chain (MRLC) at Ser-19 and Thr-18 (Iwasaki *et al.*, 2001), and ROCK-mediated phosphorylation of myosin II generates the driving force required for cell motility and morphology (Sandquist *et al.*, 2006). In apoptotic cells, caspase-3–activated ROCK-I phosphorylates myosin II excessively (Leverrier and Ridley, 2001). As a result, the hyperphosphorylated myosin II displays dramatically increased motor activity and consequently induces apoptotic membrane blebbing and apoptotic body formation (Mills *et al.*, 1998).

In mammalian cells, the activity of myosin II is counteracted by myosin phosphatase (MP; Alessi *et al.*, 1992). MP is a trimeric holoenzyme, consisting of a 38-kDa catalytic subunit, a 110-kDa myosin-binding subunit, and a 20-kDa small subunit. The catalytic subunit is the δ isoform of type 1 protein phosphatase (PP1cδ; also called PP1cβ). The small subunit is a splicing variant of the 110-kDa myosin-binding subunit, which has been suggested to interact with the microtubules (Mabuchi *et al.*, 1999; Takizawa *et al.*, 2003). The myosin-binding subunit, also referred to as the myosin phosphatase targeting subunit 1 (MYPT1), is a key regulator for MRLC dephosphorylation, which shortens the molecular distance between the phosphatase and myosin II (Terrak *et al.*, 2004). Dephosphorylation of myosin II by MP is necessary for the relaxation of actomyosin fibers in the cells. Inhibition of MP is involved in hypertension caused by vascular smooth muscle hypercontraction (Seko *et al.*, 2003). It was found that mutations of MYPT were embryonic lethal in *Caenorhabditis elegans* and *Drosophila*, because of defects in morphogenesis (Wissmann *et al.*, 1999; Mizuno *et al.*, 2002).

Proper dephosphorylation by MP is important for the myosin-mediated processes in nonapoptotic cells. However, the existence of a dephosphorylation pathway would prevent the hyperphosphorylation of myosin II in apoptotic cells. To analyze the activity of MP during apoptosis, we investigated biochemical modifications of MYPT1 in apoptotic cells. Our experimental results revealed that MYPT1 in apoptotic HeLa cells was cleaved by caspase-3, and the cleaved fragment was strongly phosphorylated at Thr-669 and Thr-853. In addition, MYPT1 in apoptotic cells neither interacted with myosin II in vitro nor colocalized with the stress fibers. MP precipitated from the apoptotic cells showed reduced myosin II dephosphorylation activity. These results suggest that inhibition of MP activity assists in inducing apoptotic membrane blebbing by reinforcing myosin II hyperphosphorylation.

RESULTS

Apoptotic cleavage of MYPT1 by caspase-3

To understand the molecular nature of MP during apoptosis, we analyzed how MYPT1 is modified in apoptotic cells. First, we compared the endogenously expressed MYPT1 in nonapoptotic and apoptotic cells by immunoblotting. As shown in Figure 1A, the antibody against MYPT1 recognized another size of protein band (lane 2, open arrowhead) in the extract of HeLa cells treated with tumor

necrosis factor-α and cycloheximide (TNF/CHX), suggesting the induction of apoptosis led to the cleavage of MYPT1. The cleavage of MYPT1 occurred n parallel with the cleavage of poly-ADP ribose polymerase (Figure 1B, lane 2, middle panel), a well-characterized caspase-3 substrate. These cleavages were inhibited when the nonselective caspase inhibitor zVAD-FMK was present during the induction of apoptosis, whereas MYPT1 was cleaved in the presence of caspase-8 inhibitor IETD-CHO (Figure 1B, lanes 3 and 4). The caspase-8 substrate BID was also weakly cleaved in IETD-CHO treatment (Figure 1B, lane 4, bottom panel), because BID is cleaved by other caspases (Slee *et al.*, 2000). The cleavage of MYPT1 was observed in another apoptosis inducer, Fas antibody, and also in the T-lymphocyte Jurkat cell (Supplemental Figure S1). These results suggest that MYPT1 is ubiquitously cleaved in apoptotic cells.

Next we performed an in vitro cleavage assay to determine which caspase was responsible for the cleavage of MYPT1 in apoptotic cells. For this purpose, the FLAG-tagged MYPT1, expressed in vitro using the wheat germ cell-free protein synthesis system, was first incubated with either the major initiator caspase (caspase-8) or the downstream executioner caspase (caspase-3), and the reaction mixture was subsequently analyzed by immunoblot assay using the anti-FLAG antibody. As shown in Figure 1B, the FLAG-MYPT1 treated with caspase-3 showed slightly increased mobility (Figure 1C; compare lanes 1 and 2). In contrast, a faster-migrating (~ 50 kDa) band was observed in FLAG-MYPT1 treated with caspase-8 (Figure 1C, lane 3, asterisk). Although the low-molecular-weight fragment observed in apoptotic cell lysate was slightly faster than the caspase-8–mediated fragment, MYPT1 might be additionally cleaved at the amino-terminal region by another protease (Figure 1A, lane 2). These results suggest that MYPT1 is at least processed by caspase-3 in vivo.

The caspase-3 cleavage site in MTPY1 was confirmed by amino acid sequencing. Because the epitope tag used in Figure 1B was fused to the amino terminus of MYPT1, we estimated that the caspase-3 cleavage site would be located near the carboxy-terminal end of MYPT1. To obtain the caspase-3–cleaved fragment of MYPT1, we recombinantly expressed MYPT1-(783-1004)–glutathione *S*-transferase (MYPT1-(783-1004)-GST), as described in *Materials and Methods*. This C-terminal portion of MYPT1 was chosen because it contained a putative caspase-3 recognition site (Mahrus *et al.*, 2008). The purified MYPT1-(783-1004)-GST was then treated with caspase-3 in vitro, and the GST-fused fragment obtained was subjected to amino acid sequence analysis. The first N-terminal residue of this cleaved fragment was identified to be Ser-885; therefore the amino acid sequence TQTD884, was confirmed as the caspase-3 recognition sequence in MYPT1. This result suggests that the 112-kDa native MYPT1 is cleaved into 98-kDa and 14-kDa fragments by caspase-3.

To confirm that caspase-3 cleaves MYPT1 at Asp-884 in vivo, we constructed a series of expression vectors encoding amino-terminally V5-tagged mouse MYPT1 (Figure 1D). HeLa cells transiently expressing the wild-type MYPT1 (V5-MYPT1-WT), caspase-3 cleavage site mutant of MYPT1 (V5-MYPT1-D884A), and the caspase-3 truncated form of MYPT1 (V5-MYPT1-(1-884)) were treated with TNF/CHX, and cell lysates were then analyzed by immunoblot using the anti-V5 antibody. Cleavage of MYPT1 was seen in the lysate of apoptotic cells expressing V5-MYPT1-WT (Figure 1E, lane 2, open arrowhead). However, this cleavage was not seen in the lysate of apoptotic cells expressing V5-MYPT1-D884A (Figure 1E, lane 4). V5-MYPT1-(1-884) was insensitive to endogenous caspase, as the migration of the expressed protein band in apoptotic cells was the same as that in nonapoptotic cells (Figure 1E, lanes 5 and 6). Taken together, these results indicate that, in apoptotic cells, caspase-3 cleaves MYPT1 at Asp-884. Because Asp-884 is located in the middle of the myosin-binding site (Figure 1D), our results also suggest that the caspase-3–mediated cleavage of MYPT1 could disrupt the interaction of myosin II with MP during apoptosis.

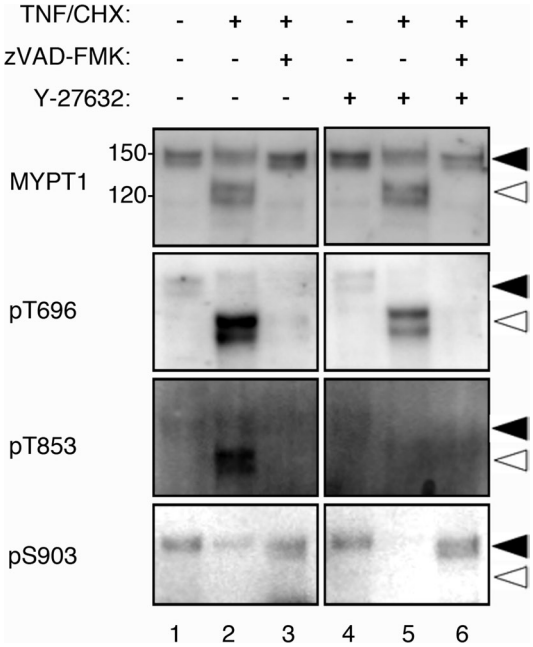

FIGURE 2: Phosphorylation of MYPT1 during apoptosis. HeLa cells were treated with DMSO, TNF/CHX, or TNF/CHX /zVAD-FMK plus Y-27632 for 3 h. Phosphorylation of endogenous MYPT1 was determined using the indicated antibody (pT696, anti–phospho-Thr-696; pT853, anti–phospho-Thr-853; or pS903, anti–phospho-Ser-903 antibody). The full-length and caspase-3–cleaved MYPT1s are indicated using filled and open arrowheads, respectively.

Phosphorylation of MYPT1 during apoptosis

It is known that phosphorylation of MYPT1 is important for the inactivation of MP. Phosphorylation of MYPT1 at Thr-696 directly inhibits the activity of MP for myosin II, whereas phosphorylation of MYPT1 at Thr-853 causes dissociation of MYPT1 from myosin II (MacDonald *et al.*, 2001; Velasco *et al.*, 2002). However, nothing is known about the phosphorylation state of MYPT1 during apoptosis. To further investigate the regulation of MYPT1 in apoptosis, we analyzed HeLa cell lysates treated with TNF/CHX by immunoblot, using antibodies against phosphorylated MYPT1 (Figure 2). Phosphorylation of MYPT1 at Thr-696 was not detected in control nonapoptotic cell lysate, but significant phosphorylation of Thr-696 was observed in apoptotic cell lysate (Figure 2, pT696, lane 2, open arrowhead). Treatment of cells with the ROCK inhibitor Y-27632 during the induction of apoptosis partly reduced the phosphorylation of Thr-696 (Figure 2, pT696, lane 5, open arrowhead), suggesting that ROCK might be involved, at least partially, in the phosphorylation of Thr-696 in MYPT1. Phosphorylation of Thr-696 of MYPT1, however, was completely inhibited by addition of zVAD-FMK during treatment with TNF/CHX (Figure 2, pT696, lanes 3 and 6), suggesting that the apoptotic phosphorylation of MYPT1 at Thr-696 is dependent on caspase activation. Similarly, significant phosphorylation of MYPT1 at Thr-853 was observed in apoptotic cells (Figure 2, pT853, lane 2, open arrowhead), but not in zVAD-FMK–treated cells (Figure 2, pT853, lane 3). Y-27632 treatment, however, completely inhibited the Thr-853 phosphorylation, which was in contrast to what we have observed with the Thr-696

residue, thus suggesting that Thr-853 is a ROCK-specific phosphorylation site (Figure 2, pT853, lane 5, open arrowhead). Phosphorylation of Thr-853 was also inhibited by zVAD-FMK treatment, suggesting that the phosphorylation of Thr-853 also depends on the caspase activity. Because ROCK-II lacks any caspase-3 cleavage site, we suggest that ROCK-I is likely to be the kinase responsible for the phosphorylation of MYPT1 at Thr-853 in apoptotic HeLa cells. Interestingly, despite the presence of full-length MYPT1 after the induction of apoptosis (Figure 2, MYPT1), only caspase-3–cleaved MYPT1 was preferentially phosphorylated at both Thr-696 and Thr-853. These results suggest that the cleavage of MYPT1 by caspase-3 is also important for the phosphorylation-mediated inactivation of MYPT1. The function of Ser-903 phosphorylation is unclear at present. The phosphorylation of MYPT1 at Ser-903 disappeared in the caspase-3–active cells, because the carboxy terminus of MYPT1 was cleaved off (Figure 2, pS903, lanes 1 and 2, open arrowhead).

Dissociation of MYPT1 from myosin II during apoptosis

To examine whether the apoptotic modifications have any effect on the myosin-binding activity of MYPT1, we performed a coimmunoprecipitation assay using HeLa cell lysates expressing V5-MYPT1-WT. Myosin II was found to precipitate along with MYPT1 in the immunoprecipitate prepared from the nonapoptotic cell lysate using the anti-V5 antibody (Figure 3A, lane 5, asterisk). In contrast, myosin II was not found in the immunoprecipitate from the lysate of apoptotic cells (Figure 3A, lane 6). These results suggest that MYPT1 in apoptotic cells does not interact with myosin II. V5-MYPT1 precipitated from the cells contained both the intact and cleaved forms (Figure 3A, lanes 5 and 6). To further clarify the dissociation of myosin II from cleaved MYPT1, we performed a pull-down assay from HeLa cell lysates, using FLAG-MYPT1 synthesized by the wheat germ cell-free system (Figure 3B). According to the in vivo results, myosin II was precipitated with FLAG-MYPT1-WT/T696AT853A, but not with FLAG-MYPT1-(1-884)/T696AT853A-(1-884) (Figure 3B, lanes 2–5). As demonstrated in Figure 2, we observed apoptotic phosphorylations of MYPT1, which decrease the myosin II–binding activity (Velasco *et al.*, 2002). It is noteworthy that the pseudophosphorylated mutants, FLAG-MYPT1-T696DT853D and FLAG-MYPT1-T696DT853D-(1-884) did not interact with myosin II (Figure 3B, lanes 6 and 7). Taken together, cleavage of myosin-binding domain and phosphorylation of Thr-696/Thr-853 are important for the dissociation of myosin II from MYPT1, and the combination of these modifications may further reduce the myosin II–binding activity of MYPT1.

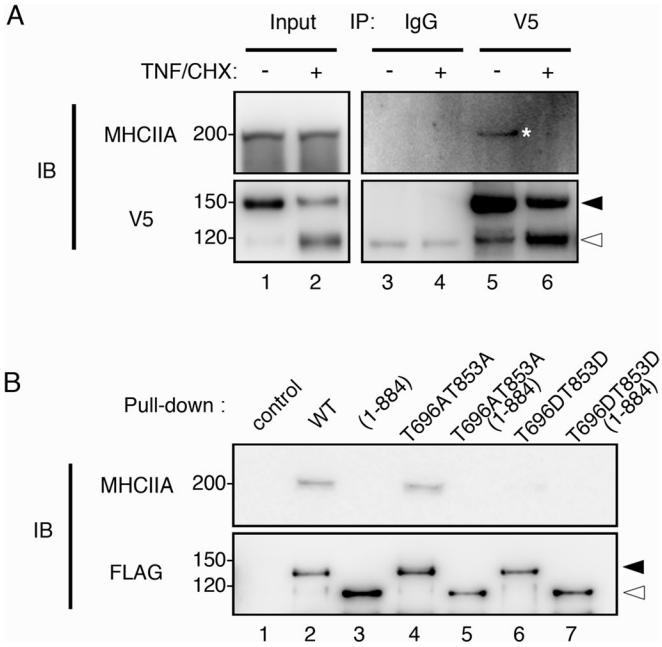

FIGURE 3: Dissociation of MYPT1 from myosin II during apoptosis. (A) HeLa cells expressing V5-MYPT1-WT were treated with DMSO or TNF/CHX for 3 h. Immunoprecipitates prepared with anti-mouse immunoglobulin G (IgG, lanes 3 and 4) and anti-V5 antibody (V5, lanes 5 and 6), respectively, were immunoblotted with anti–myosin heavy chain IIA antibody (MHCIIA). (B) Pull-down assay from nonapoptotic HeLa cell lysates was performed using FLAG-MYPT1-WT, FLAG-MYPT1-(1-884), FLAG-MYPT1-T696AT853A, FLAG-MYPT1-T696AT853A-(1-884), FLAG-MYPT1-T696DT853D, and FLAG-MYPT1-T696DT853D-(1-884), respectively (lanes 2–7). The precipitates were probed with anti–myosin heavy chain IIA antibody (MHCIIA). Filled and open arrowheads indicate the positions of full-length and caspase-3–cleaved MYPT1, respectively.

Localization of caspase-3 cleaved MYPT1

In cultured mammalian cells, MYPT1 localizes at stress fibers (Kawano *et al.*, 1999). Localization of MYPT1 at stress fibers is important for the dephosphorylation of myosin II by MP. As the localization of MYPT1 in apoptosis is not known, we transiently transfected HeLa cells with V5-MYPT1-WT–, V5-MYPT1-D884A–, and V5-MYPT1-(1-884)–expressing vector, respectively, and subsequently stained the cells with anti-V5 antibody, anti-myosin heavy chain IIA antibody, and phalloidin (Figure 4). As shown, V5-MYPT1-WT and V5-MYPT1-D884A were localized at the cortical actin fiber (Figure 4, A–H). However, C-terminal–cleaved mutant of MYPT1, V5-MYPT1-(1-884), was found to be localized mainly in the nucleus, but not at stress fibers (Figure 4, I–L). Mislocalization of the V5-MYPT1-(1-884) suggests that deletion of the myosin-binding region by caspase-3 reduces the myosin-binding affinity of MYPT1. In addition, the pseudophosphorylated mutants, V5-MYPT1-T696DT853D and V5-MYPT1-T696DT853D-(1-884) also showed dissociation from stress fibers (Figure 4, M–P). On the basis of the localization of each MYPT1 mutant in the cells, we quantitatively analyzed the contribution of MYPT1 phosphorylation and cleavage to stress fiber localization. In V5-MYPT1-WT–expressing cells, more than 83% of the cells showed stress fiber localization of MYPT1, whereas the localization at stress fibers was dramatically decreased in V5-MYPT1-T696DT853D-(1-884)–expressing cells. V5-MYPT1-(1-884) and V5-MYPT1-T696DT853D showed intermediate values. These results suggest that concomitant phosphorylation and cleavage is important for efficient dissociation of MYPT1 from stress fibers.

In apoptotic HeLa cells, both V5-MYPT1-WT and V5-MYPT1-D884A showed increased cytoplasmic diffusion and faint localization at the cortex (unpublished data). Because of high background caused by cell shrinkage in apoptosis, it was difficult to distinguish between the localization of V5-MYPT1-WT and V5-MYPT1-D884A.

Apoptotic dephosphorylation of myosin II by MP

The observed reduction in the myosin-binding activity of MYPT1 in apoptotic cells suggests that the activity of MP might be reduced during apoptosis. For testing this hypothesis, endogenous MP containing PP1cδ was immunoprecipitated from the cell lysates of nonapoptotic and apoptotic cells, using anti-MYPT1 antibody (Figure 5A, lanes 1 and 2), and the phosphatase activity of the immunoprecipitated MP was analyzed in vitro. Myosin II was first phosphorylated by zipper-interacting protein kinase (ZIPK; Murata-Hori *et al.*, 1999). Dephosphorylation of myosin II

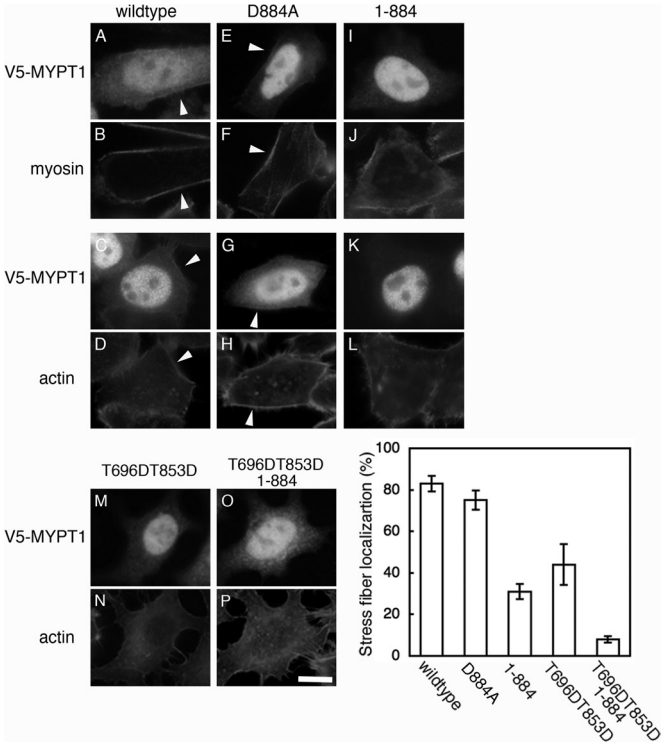

FIGURE 4: Localization of caspase-3–cleaved MYPT1. HeLa cells transiently transfected with V5-MYPT1-WT (A–D), V5-MYPT1-D884A (E–H), V5-MYPT1-(1-884) (I–L), V5-MYPT1-T696DT853D (M and N), and V5-MYPT1-T696DT853D-(1-884) (O and P) were doubly stained with anti-V5 antibody and either with anti–myosin heavy chain IIA antibody or with phalloidin. Localization of MYPT1 at the cortex region is indicated by white arrowheads. Scale bar: 30 μm. Graph shows percentage of the cells in which V5-MYPT1 is localized at stress fibers. Results shown are mean ± SD of three independent experiments.

at indicated times by MP was then analyzed by immunoblot, using the anti–Ser-19 phosphorylated MRLC antibody (Figure 5B). During the initial phase of the dephosphorylation reaction (up to 3 min), the MP from the apoptotic HeLa cells showed ~30% lower activity than that from the nonapoptotic cells. However, at longer incubation times (10–30 min), the amount of dephosphorylated myosin II generated by the MPs was not significantly different in apoptotic versus nonapoptotic cells. This result suggests that apoptotic modifications of MYPT1 affect the dephosphorylation efficiency in the short term but not the phosphatase activity itself. Intense membrane blebbing has been reported to be completed within approximately 10 min (Lane *et al.*, 2005); the lower activity of MP at the initial phase of apoptosis might be related to this phenomenon.

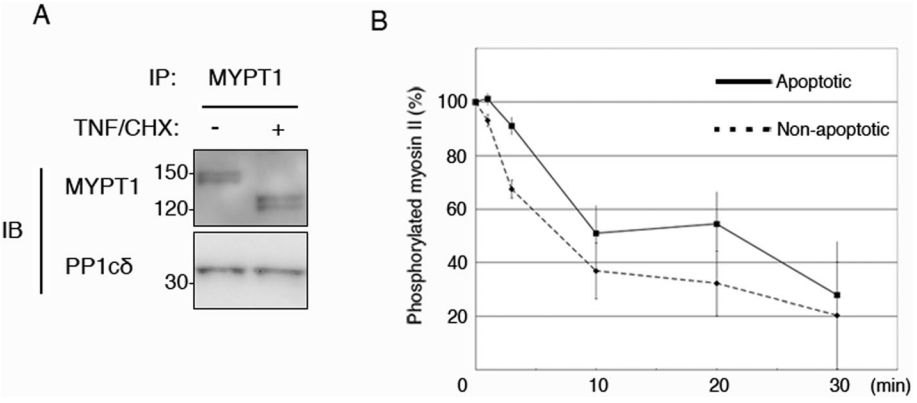

FIGURE 5: Phosphatase activity of apoptotic MP. MP was immunoprecipitated by anti-MYPT1 antibody from nonapoptotic cells (A, lane 1) and apoptotic cells (A, lane 2). Coimmunoprecipitation of MP component was confirmed by anti-PP1cδ antibody. Myosin II, phosphorylated with ZIPK, was incubated with apoptotic (B, solid line) and nonapoptotic (B, dotted line) MPs for the indicated times. Remaining amount of phosphorylated myosin II was determined using anti–Ser-19 phosphorylated MRLC antibody. Each data point represents mean ± SD of three independent experiments.

Effect of MYPT1 knockdown on apoptosis

To further understand the function of MYPT1 during apoptosis, we examined the MYPT1 knockdown by RNA interference. Immunoblot analysis revealed that 48-h treatment of HeLa cells with human MYPT1-specific small interfering RNA (siRNA) reduced the expression level of MYPT1 to 25% of the control cells (Figure 6A, lanes 1 and 2). As reported previously (Wu *et al.*, 2010), knockdown of MYPT1 did not cause apoptosis in normal HeLa cells. However, the percentage of TNF/CHX-induced apoptotic cells was increased in MYPT1-depleted cells (Figure 6B). Quantitative analysis by fluorescein isothiocyanate (FITC)-annexin V and propidium iodide (PI) staining revealed that the percentage of apoptotic cells increased from 14 to 25% (3 h after treatment with TNF/CHX), and 58 to 78% (6 h after treatment with TNF TNF/CHX). Because of the DNA sequence difference, the expression of mouse-derived V5-MYPT1-WT was not knocked down by human MYPT1-specific siRNA. Therefore we performed a rescue experiment by cotransfecting HeLa cells with MYPT1 siRNA and V5-MYPT1-WT vector (Figure 6A, lane 3). Coexpression of V5-MYPT1-WT reduced, at least partially, the percentage of apoptotic cells (15% in 3 h and 64% in 6 h) in HeLa cells. In TNF/CHX/zVAD-FMK–treated cells, the percentage of apoptotic cells was not statistically significant under scrambled siRNA-treated, MYPT1 siRNA-treated, and MYPT1 rescue conditions. These results suggest that MYPT1 depletion reduces cells' ability to resist against apoptosis.

DISCUSSION

Since 1994, a large number of proteins have been identified as substrates for caspase-3 (Fernandes-Alnemri *et al.*, 1994). Among these substrates, cleavage of cytoskeleton-related proteins could cause critical cellular dysfunction. During the initial phase of this study, we screened for caspase-3–cleaved proteins responsible for myosin II phosphorylation and dephosphorylation. For screening, we combined our wheat germ protein expression system with an in vitro caspase cleavage assay. In general, cell-based protein synthesis requires several steps, including vector construction, gene expression, and protein purification from the cell. In contrast, our cell free–based protein expression method can synthesize multiple proteins by cDNA amplification and in vitro translation and transcription (Takai *et al.*, 2010). Moreover, the synthesized protein containing wheat germ extract can be directly used in the caspase assay, because of the protease-free environment. Using this method, we have produced a protein library containing 304 kinases, and we have screened this

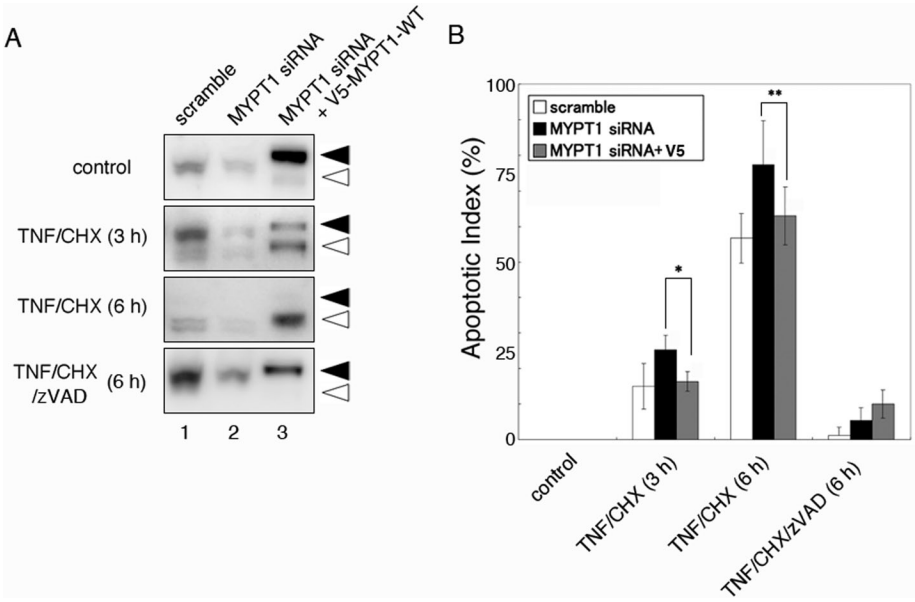

FIGURE 6: Effect of MYPT1 depletion on apoptotic cells. (A) HeLa cells were transfected with scrambled siRNA (lane 1), human MYPT1 siRNA (lane 2), or human MYPT1 siRNA and V5-MYPT1-WT vector (lane 3). Forty-eight hours after transfection, the cells were treated with DMSO, TNF/CHX, or TNF/CHX/zVAD-FMK for the indicated times. Total cell lysates were immunoblotted with anti-MYPT1 antibody. The full-length and caspase-3–cleaved MYPT1s are indicated using filled and open arrowheads, respectively. (B) The dead cells in the indicated time were counted after staining the cells with FITC-annexin V and PI. The apoptotic index was calculated by determining the percentage of dead cells in the field (n = 100–200). Results shown are mean ± SD of four independent experiments. Statistical significance was determined using Student's t test (*, $p < 0.005$; **, $p < 0.05$).

library to identify 30 novel caspase-3–sensitive kinases. It is noteworthy that the caspase-3–cleaved novel myosin II kinase was not detected by this assay (Tadokoro *et al.*, 2010). Using this assay, we also detected cleavage of the MYPT homologues MYPT3 and MBS85 by caspase-3 in vitro (unpublished data). Although the biological functions of these MYPT homologues are not yet clear, both homologues were found to be highly expressed in multiple tissues, including heart and brain (Skinner and Saltiel, 2001; Dutheil *et al.*, 2004). Therefore MP inactivation by cleavage of MYPT homologues might be an important apoptosis-related process involved in tissue development.

As shown in Figure 2, we have found that ROCK-I was responsible for the apoptotic phosphorylation of MYPT1 at Thr-853. The apoptotic phosphorylation of MYPT1 at Thr-696, however, was not completely inhibited by Y-27632, suggesting that Thr-696 is phosphorylated by several apoptosis-activated kinases, including ROCK. A previous study showed that smooth muscle MYPT1 was phosphorylated at Thr-696 by ZIPK in vitro (MacDonald *et al.*, 2001). ZIPK is a member of the death-associated protein kinase family, which is known to induce apoptotic cell death (Murata-Hori *et al.*, 2001). These reports suggest the possibility that ZIPK could be a candidate kinase involved in the apoptotic phosphorylation of MYPT1. Inactivation of MP due to MYPT1 phosphorylation is also reported in mitotic cells and tetradecanoylphorbol-13-acetate–treated cells (Kawano *et al.*, 1999; Totsukawa *et al.*, 1999). Therefore down-regulation of MP through MYPT1 phosphorylation is a ubiquitous event for myosin II activation in apoptosis, cytokinesis, and cell migration. It is noteworthy, however, that the activity of MP is more strictly down-regulated by additional cleavage of MYPT1 in apoptosis.

It is known that MP is localized not only at stress fibers but also in the nucleus. We have found that cleavage by caspase-3 did not affect the nuclear localization of MYPT1 (Figure 4), and this result was consistent with the previous report that the N-terminus of MYPT1 is important for its transport to the nucleus (Wu *et al.*, 2005). The function of nuclear MP is not clear, however, because of the absence of myosin II in the nucleus. One possibility is that the nucleus is working as storage for MP to regulate the phosphorylated myosin II in the cytoplasm. In fact, following the nuclear envelope breakdown in the mitotic phase, MYPT1 strongly colocalized with the phosphorylated myosin II at the cleavage furrow (Kawano *et al.*, 1999). Based on this information, it was assumed that the nuclear MP is released into the cytoplasm by apoptotic nuclear degradation. In support of this assumption, it was observed that the amount of soluble PP1cδ increases during apoptosis (Puntoni and Villa-Moruzzi, 1999). Therefore dysfunction of MYPT1 may be important to maintain the phosphorylation level of myosin II in apoptotic cells. Although dephosphorylation of myosin II is a dispensable pathway for apoptotic membrane blebbing, the activity of PP1 is essential for apoptotic progression. PP1 itself does not have any specific substrate, but it enables dephosphorylation of multiple substrates by interacting with various regulatory subunits. In the apoptotic pathway, apoptosis-related proteins, such as Bcl-2, BAD, and caspases, are activated by PP1-mediated dephosphorylation (Mukerjee *et al.*, 2001; Ruvolo *et al.*, 2001). The dysfunction of MYPT1 and release of PP1cδ might be concomitantly occurring in the apoptotic cells.

Our proposed model for myosin II hyperphosphorylation during apoptosis is shown in Figure 7. Until now, the apoptotic hyperphosphorylation of myosin II and the subsequent membrane blebbing were simply thought to be caused by the caspase-3–mediated activation of ROCK-I. In the present study, we have identified MYPT1 as a novel substrate for caspase-3, and we also have shown that MYPT1 was phosphorylated at Thr-696 and Thr-853 during apoptosis. These apoptotic modifications of MYPT1 in turn decreased the phosphatase activity of MP for myosin II. Our findings, however, do not interfere with the current model of apoptosis involving myosin II phosphorylation, but suggest further augmentation of apoptotic phosphorylation of myosin II for apoptotic membrane blebbing. Generally, membrane blebbing is a ubiquitous phenomenon observed during cell migration, cell spreading, cytokinesis, and apoptosis (Fackler and Grosse, 2008). However, the apoptotic membrane blebbing is specifically distinguished from the vital blebbing by irreversibility and durability. In addition, the apoptotic membrane blebbing finally tears the dying cell into small apoptotic bodies. However, the apoptotic blebbing under caspase inhibitory condition is not strong enough to pinch off the apoptotic body (McCarthy *et al.*, 1997), thus suggesting the importance of myosin II activation in apoptosis. After the exclusion of apoptotic bodies from the tissue, neighboring cells stretch and supplement the gapped space (Peralta Soler *et al.*, 1996). The underlying mechanism that detects the opened space and repairs the tissue is, however, still unclear. It

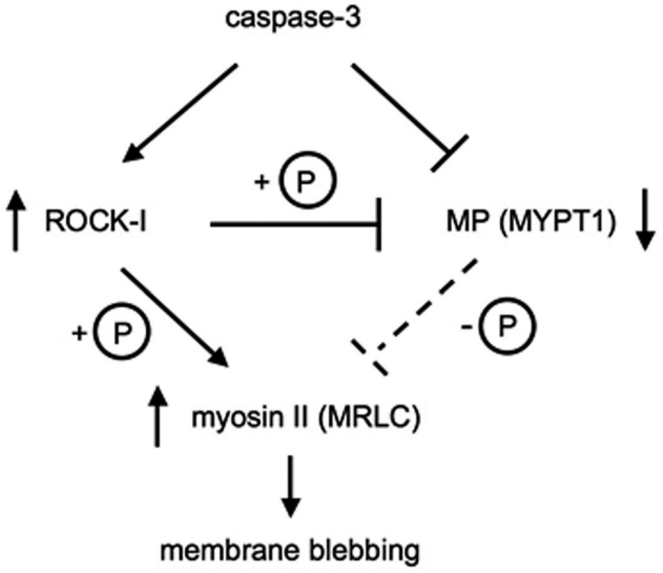

FIGURE 7: Model proposed for the regulation of myosin II hyperphosphorylation in apoptosis.

was previously shown in monolayer epithelial cells that the phosphorylation level of myosin II is increased by physiological stimulation (Birukov *et al.*, 2003). In apoptosis, living cells surrounding the apoptotic cell would be expected to undergo continuous stimulation when blebbing is significant. Although further studies are required to understand whether the apoptotic membrane blebbing has any additional function, one could imagine that intense apoptotic blebbing might contribute by initiating migration of the surrounding cells via stimulation-induced myosin II phosphorylation.

MATERIALS AND METHODS

Drugs and antibodies

Rabbit polyclonal antibody against phospho–Thr-853 MYPT1 was purchased from Cell Signaling Technology (Danvers, MA). Rabbit polyclonal antibodies against phospho–Thr-696 MYPT1 and PP1cδ were purchased from Millipore (Billerica, MA). Rabbit polyclonal antibodies against MYPT1 (H-130) and phospho–Ser-903 MYPT1 were purchased from Santa Cruz Biotechnology (Santa Cruz, CA). All other materials used in this study were reagent grades.

Plasmid construction

Mouse MYPT1 cDNA (MGI:1309528) was obtained from the FANTOM full-length cDNA clone collection (RIKEN, Tsukuba Japan). Mutant MYPT1 cDNAs, termed as MYPT1-D884A, MYPT1-(1-884), MYPT1-T696AT853A, MYPT1-T696AT853A-(1-884), MYPT1-T696DT853D, and MYPT1-T696DT853D-(1-884) were generated by PCR. Using the Gateway cloning technology (Invitrogen, Carlsbad, CA), cDNAs were individually subcloned into pEU-E01-GW for cell-free protein expression and into pcDNA3.1/nV5-DEST for expression in mammalian cells.

Wheat germ cell-free protein synthesis and in vitro caspase cleavage assay

In vitro transcription and cell-free protein synthesis were carried out as described previously (Takahashi *et al.*, 2009). Briefly, mRNA for protein synthesis was prepared from the FLAG-tagged mouse MYPT1 cDNA amplified by PCR. The translation reaction was carried out for 18 h at 16°C with a bilayer method using the ENDEXT technology kit (CellFree Sciences, Matsuyama, Japan). For the caspase cleavage assay, 1 mU of caspase-3 (Sigma-Aldrich, St. Louis, MO) was added to the protein synthesis mixture and incubated for 1 h at 30°C. The protein mixture treated with caspase was separated on SDS–PAGE and then subjected to immunoblot assay using the anti-FLAG monoclonal antibody (Sigma-Aldrich). Cleavage of FLAG-MYPT1 was detected using the ECL plus Western Blotting Reagent kit and a Typhoon Imager (GE Healthcare, Buckinghamshire, UK).

Amino acid sequencing

MYPT1-(783-1004) cDNA was generated by PCR and subcloned into pGEX-5X for expression in *Escherichia coli*. The expressed GST fusion protein was purified using glutathione Sepharose beads and then treated with caspase-3. The caspase-3–cleaved fragment was separated on SDS–PAGE and was analyzed with the Procise 491 protein sequencer (Applied Biosystems, Carlsbad, CA).

Cell culture and drug treatment

HeLa cells (RCB0007) were obtained from the RIKEN Cell Bank and cultured at 37°C with 5% CO_2 in DMEM supplemented with 10% fetal bovine serum, 100 U/ml penicillin, and 100 μg/ml streptomycin. Transfection was performed using Lipofectamine 2000 reagent (Invitrogen) according to the manufacturer's instructions. For inducing apoptosis, cells were treated with 20 ng/ml of TNF-α and 100 μM of CHX (Calbiochem, La Jolla, CA). ZVAD-FMK (Peptide Institute, Osaka, Japan) and Y-27632 (Calbiochem) were added to a final concentration of 100 μM and 10 μM, respectively, during apoptosis induction.

Immunoblot and immunoprecipitation assays

HeLa cells, treated with or without TNF/CHX, were washed with phosphate-buffered saline (PBS) and lysed with Laemmli sample buffer (Laemmli, 1970), and then the cell lysates were subjected to immunoblot assay. Briefly, after blocking with 3% non-fat milk, membranes were probed with a given primary antibody; this was followed by the horseradish peroxidase (HRP)-conjugated secondary antibodies. The blots were visualized using the Immobilon Western Chemiluminescent HRP Substrate (Millipore) and LAS-3000 mini-image analyzer (Fujifilm, Tokyo, Japan). For immunoprecipitation, V5-MYPT1 transfected HeLa cells were washed with PBS and resuspended in ice-cold lysis buffer containing 30 mM Tris-HCl (pH 7.5), 150 mM NaCl, 1 mM EDTA, 1% Triton X-100, 0.5% NP-40, supplemented with protease inhibitor, and phosphatase inhibitor cocktail (Sigma-Aldrich). Cells were lysed by passing them through an 18-gauge needle, and the lysate was clarified by centrifugation at 8000 × *g* for 10 min at 4°C. The cell lysate was incubated with anti-V5 antibody bound to Dynabeads Protein G (Invitrogen) under constant rotation for 1 h. The beads were washed three times with the lysis buffer and then the immunoprecipitate was eluted off the beads with V5-peptide (Sigma-Aldrich).

Indirect immunofluorescence

Indirect immunofluorescence was carried out as described previously (Murata-Hori *et al.*, 2001). Briefly, cells grown on coverslips were fixed with 3.7% formaldehyde and then permeabilized with 0.2% Triton X-100. After being blocked with 1% bovine serum albumin in PBS for 30 min, cells were stained with mouse anti-V5 antibody or rabbit anti–myosin heavy chain IIA antibody for 1 h; this was followed by Alexa Fluor 488–conjugated secondary antibody, Alexa Fluor 555–conjugated phalloidin, and 4′,6-diamidino-2-phenylindole. Cells were mounted onto a microscope slide with a drop of SlowFade (Invitrogen) to preserve fluorescence. Imaging was

performed on an Olympus DP50 (Tokyo, Japan). All images were processed with custom software.

MP assay

Smooth muscle myosin II was purified from chicken gizzard as previously described (Ebashi, 1976). For preparation of phosphorylated myosin II, purified myosin II was incubated with GST-ZIPK in 100 mM Tris-HCl (pH 7.5), 50 mM $MgCl_2$, and 0.5 mM ATP for 60 min at 25°C (Murata-Hori *et al.*, 1999). After phosphorylation, GST-ZIPK binding to glutathione beads was removed by centrifugation. MP was immunoprecipitated from the HeLa cells using anti-MYPT1 antibody. Equal amounts of immunoprecipitated MP were incubated with 0.5 mM phosphorylated myosin II for the indicated times at 30°C. The reaction was terminated by the addition of Laemmli sample buffer, and the mixture was subjected to SDS–PAGE. The amount of phosphorylated myosin II was determined by immunoblot using phospho–Ser-19 MRLC antibody (Millipore).

RNA interference

Predesigned siRNA against human MYPT1 and scrambled siRNA was obtained from Dharmacon (Lafayette, CO). SiRNA was transfected into the HeLa cells with Lipofectamine 2000 for 48 h before apoptosis induction. To rescue MYPT1 expression, we used the V5-MYPT1-WT vector for cotransfection along with the siRNA. The cells treated with TNF/CHX were stained with FITC-annexin V (BD PharMingen, Franklin Lakes, NJ) and PI and then counted under a microscope.

ACKNOWLEDGMENTS

We thank Masayuki Takahashi (University of Hokkaido) for kindly providing anti–myosin heavy chain IIA antibody. This work was supported in part by a Grant-in-Aid for Scientific Research (B) (T.S.), a Grant-in-Aid for Young Scientists (21870029 to T.I.) from the Japan Society for the Promotion of Science, and a Grant-in-Aid for Scientific Research on Innovative Areas (T.S.) from the Ministry of Education, Culture, Sports, Science and Technology, Japan.

REFERENCES

Alessi D, MacDougall LK, Sola MM, Ikebe M, Cohen P (1992). The control of protein phosphatase-1 by targetting subunits. The major myosin phosphatase in avian smooth muscle is a novel form of protein phosphatase-1. Eur J Biochem 210, 1023–1035.

Birukov KG, Jacobson JR, Flores AA, Ye SQ, Birukova AA, Verin AD, Garcia JG (2003). Magnitude-dependent regulation of pulmonary endothelial cell barrier function by cyclic stretch. Am J Physiol Lung Cell Mol Physiol 285, L785–L797.

Coleman ML, Sahai EA, Yeo M, Bosch M, Dewar A, Olson MF (2001). Membrane blebbing during apoptosis results from caspase-mediated activation of ROCK I. Nat Cell Biol 3, 339–345.

Dutheil N, Yoon-Robarts M, Ward P, Henckaerts E, Skrabanek L, Berns KI, Campagne F, Linden RM (2004). Characterization of the mouse adeno-associated virus AAVS1 ortholog. J Virol 78, 8917–8921.

Ebashi S (1976). A simple method of preparing actin-free myosin from smooth muscle. J Biochem 79, 229–231.

Fackler OT, Grosse R (2008). Cell motility through plasma membrane blebbing. J Cell Biol 181, 879–884.

Fernandes-Alnemri T, Litwack G, Alnemri ES (1994). CPP32, a novel human apoptotic protein with homology to *Caenorhabditis elegans* cell death protein Ced-3 and mammalian interleukin-1 beta-converting enzyme. J Biol Chem 269, 30761–30764.

Friedlander RM (2003). Apoptosis and caspases in neurodegenerative diseases. N Engl J Med 348, 1365–1375.

Ghavami S *et al.* (2009). Apoptosis and cancer: mutations within caspase genes. J Med Genet 46, 497–510.

Iwasaki T, Murata-Hori M, Ishitobi S, Hosoya H (2001). Diphosphorylated MRLC is required for organization of stress fibers in interphase cells and the contractile ring in dividing cells. Cell Struct Funct 26, 677–683.

Jacobson MD, Weil M, Raff MC (1997). Programmed cell death in animal development. Cell 88, 347–354.

Karin M, Lin A (2002). NF-κB at the crossroads of life and death. Nat Immunol 3, 221–227.

Kawano Y, Fukata Y, Oshiro N, Amano M, Nakamura T, Ito M, Matsumura F, Inagaki M, Kaibuchi K (1999). Phosphorylation of myosin-binding subunit (MBS) of myosin phosphatase by Rho-kinase in vivo. J Cell Biol 147, 1023–1038.

Laemmli UK (1970). Cleavage of structural proteins during the assembly of the head of bacteriophage T4. Nature 227, 680–685.

Lane JD, Allan VJ, Woodman PG (2005). Active relocation of chromatin and endoplasmic reticulum into blebs in late apoptotic cells. J Cell Sci 118, 4059–4071.

Leverrier Y, Ridley AJ (2001). Apoptosis: caspases orchestrate the ROCK 'n' bleb. Nat Cell Biol 3, E91–E93.

Levkau B, Herren B, Koyama H, Ross R, Raines EW (1998). Caspase-mediated cleavage of focal adhesion kinase pp125FAK and disassembly of focal adhesions in human endothelial cell apoptosis. J Exp Med 187, 579–586.

Mabuchi K, Gong BJ, Langsetmo K, Ito M, Nakano T, Tao T (1999). Isoforms of the small non-catalytic subunit of smooth muscle myosin light chain phosphatase. Biochim Biophys Acta 1434, 296–303.

MacDonald JA, Borman MA, Murányi A, Somlyo AV, Hartshorne DJ, Haystead TA (2001). Identification of the endogenous smooth muscle myosin phosphatase-associated kinase. Proc Natl Acad Sci USA 98, 2419–2424.

Mahrus S, Trinidad JC, Barkan DT, Sali A, Burlingame AL, Wells JA (2008). Global sequencing of proteolytic cleavage sites in apoptosis by specific labeling of protein N termini. Cell 134, 866–876.

McCarthy NJ, Whyte MK, Gilbert CS, Evan GI (1997). Inhibition of Ced-3/ICE-related proteases does not prevent cell death induced by oncogenes, DNA damage, or the Bcl-2 homologue Bak. J Cell Biol 136, 215–227.

Mercer J, Helenius A (2008). Vaccinia virus uses macropinocytosis and apoptotic mimicry to enter host cells. Science 320, 531–535.

Mills JC, Stone NL, Erhardt J, Pittman RN (1998). Apoptotic membrane blebbing is regulated by myosin light chain phosphorylation. J Cell Biol 140, 627–636.

Mizuno T, Tsutsui K, Nishida Y (2002). *Drosophila* myosin phosphatase and its role in dorsal closure. Development 129, 1215–1223.

Mukerjee N, McGinnis KM, Gnegy ME, Wang KK (2001). Caspase-mediated calcineurin activation contributes to IL-2 release during T cell activation. Biochem Biophys Res Commun 285, 1192–1199.

Murata-Hori M, Fukuta Y, Ueda K, Iwasaki T, Hosoya H (2001). HeLa ZIP kinase induces diphosphorylation of myosin II regulatory light chain and reorganization of actin filaments in nonmuscle cells. Oncogene 20, 8175–8183.

Murata-Hori M, Suizu F, Iwasaki T, Kikuchi A, Hosoya H (1999). ZIP kinase identified as a novel myosin regulatory light chain kinase in HeLa cells. FEBS Lett 451, 81–84.

Peralta Soler A, Mullin JM, Knudsen KA, Marano CW (1996). Tissue remodeling during tumor necrosis factor-induced apoptosis in LLC-PK1 renal epithelial cells. Am J Physiol 270, F869–F879.

Puntoni F, Villa-Moruzzi E (1999). Protein phosphatase-1 activation and association with the retinoblastoma protein in colcemid-induced apoptosis. Biochem Biophys Res Commun 266, 279–283.

Ruvolo PP, Deng X, May WS (2001). Phosphorylation of Bcl2 and regulation of apoptosis. Leukemia 15, 515–522.

Sandquist JC, Swenson KI, Demali KA, Burridge K, Means AR (2006). Rho kinase differentially regulates phosphorylation of nonmuscle myosin II isoforms A and B during cell rounding and migration. J Biol Chem 281, 35873–35883.

Savill J, Dransfield I, Gregory C, Haslett C (2002). A blast from the past: clearance of apoptotic cells regulates immune responses. Nat Rev Immunol 2, 965–975.

Seko T, Ito M, Kureishi Y, Okamoto R, Moriki N, Onishi K, Isaka N, Hartshorne DJ, Nakano T (2003). Activation of RhoA and inhibition of myosin phosphatase as important components in hypertension in vascular smooth muscle. Circ Res 92, 411–418.

Skinner JA, Saltiel AR (2001). Cloning and identification of MYPT3: a prenylatable myosin targetting subunit of protein phosphatase 1. Biochem J 356, 257–267.

Slee EA, Adrain C, Martin SJ (2001). Executioner caspase-3, -6, and -7 perform distinct, non-redundant roles during the demolition phase of apoptosis. J Biol Chem 276, 7320–7326.

Slee EA, Keogh SA, Martin SJ (2000). Cleavage of BID during cytotoxic drug and UV radiation-induced apoptosis occurs downstream of the point of Bcl-2 action and is catalysed by caspase-3: a potential feedback loop for amplification of apoptosis-associated mitochondrial cytochrome c release. Cell Death Differ 7, 556–565.

Tadokoro D, Takahama S, Shimizu K, Hayashi S, Endo Y, Sawasaki T (2010). Characterization of a caspase-3-substrate kinome using an N- and C-terminally tagged protein kinase library produced by a cell-free system. Cell Death Dis 1, e89.

Takahashi H, Nozawa A, Seki M, Shinozaki K, Endo Y, Sawasaki T (2009). A simple and high-sensitivity method for analysis of ubiquitination and polyubiquitination based on wheat cell-free protein synthesis. BMC Plant Biol 9, 39.

Takai K, Sawasaki T, Endo Y (2010). Practical cell-free protein synthesis system using purified wheat embryos. Nat Protoc 5, 227–238.

Takizawa N, Schmidt DJ, Mabuchi K, Villa-Moruzzi E, Tuft RA, Ikebe M (2003). M20, the small subunit of PP1M, binds to microtubules. Am J Physiol Cell Physiol 284, C250–C262.

Terrak M, Kerff F, Langsetmo K, Tao T, Dominguez R (2004). Structural basis of protein phosphatase 1 regulation. Nature 429, 780–784.

Totsukawa G, Yamakita Y, Yamashiro S, Hosoya H, Hartshorne DJ, Matsumura F (1999). Activation of myosin phosphatase targeting subunit by mitosis-specific phosphorylation. J Cell Biol 144, 735–744.

Velasco G, Armstrong C, Morrice N, Frame S, Cohen P (2002). Phosphorylation of the regulatory subunit of smooth muscle protein phosphatase 1M at Thr850 induces its dissociation from myosin. FEBS Lett 527, 101–104.

Wissmann A, Ingles J, Mains PE (1999). The *Caenorhabditis elegans* mel-11 myosin phosphatase regulatory subunit affects tissue contraction in the somatic gonad and the embryonic epidermis and genetically interacts with the Rac signaling pathway. Dev Biol 209, 111–127.

Wolf D, Witte V, Laffert B, Blume K, Stromer E, Trapp S, d'Aloja P, Schürmann A, Baur AS (2001). HIV-1 Nef associated PAK and PI3-kinases stimulate Akt-independent Bad-phosphorylation to induce anti-apoptotic signals. Nat Med 7, 1217–1224.

Wu Q, Sahasrabudhe RM, Luo LZ, Lewis DW, Gollin SM, Saunders WS (2010). Deficiency in myosin light-chain phosphorylation causes cytokinesis failure and multipolarity in cancer cells. Oncogene 29, 4183–4193.

Wu Y, Murányi A, Erdodi F, Hartshorne DJ (2005). Localization of myosin phosphatase target subunit and its mutants. J Muscle Res Cell Motil 26, 123–134.